

## Electronic Supplementary Information

### Effects of Substituent, Pi-expansion and Additional Hydroxyl on the Excited State Single and Double Proton Transfer of 2-Hydroxybenzaldehyde and its Relative Compounds: TD-DFT Static and Dynamics Study

Chanatkran Prommin,<sup>†‡</sup> Khaniththa Kerdpol,<sup>†</sup> Tinnakorn Saelee,<sup>†</sup> and Nawee Kungwan<sup>†§</sup>

<sup>†</sup>*Department of Chemistry, Faculty of Science, Chiang Mai University, Chiang Mai 50200, Thailand*

<sup>‡</sup>*The Graduate School, Chiang Mai University, Chiang Mai 50200, Thailand*

<sup>§</sup>*Center of Excellence in Materials Science and Technology, Chiang Mai University, Thailand*

\*Corresponding authorE-mail :nawekung@gmail.com

Phone+ :66-53-943341 ext 126 Fax+ :66-53-892277.

**Table S1** Vibrational frequencies of the R2 stretching vibration involved in PT process of mono-PT-type both in S<sub>0</sub> and S<sub>1</sub>.

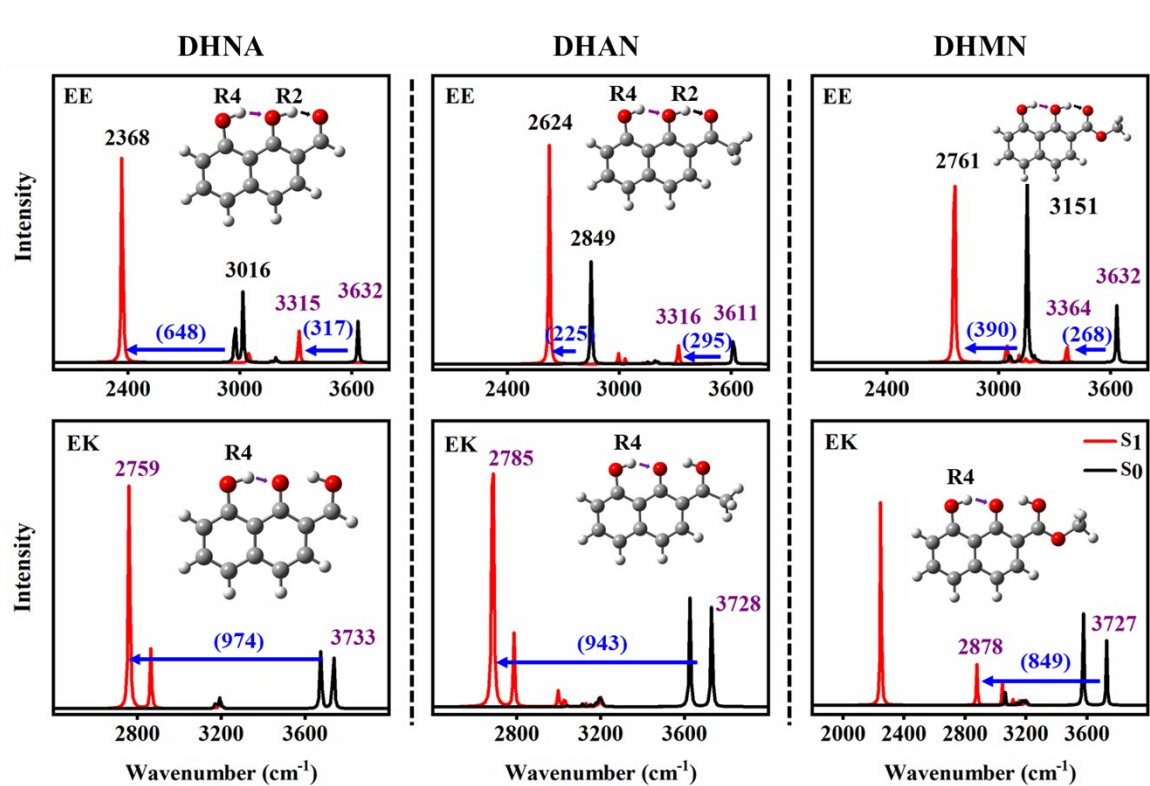
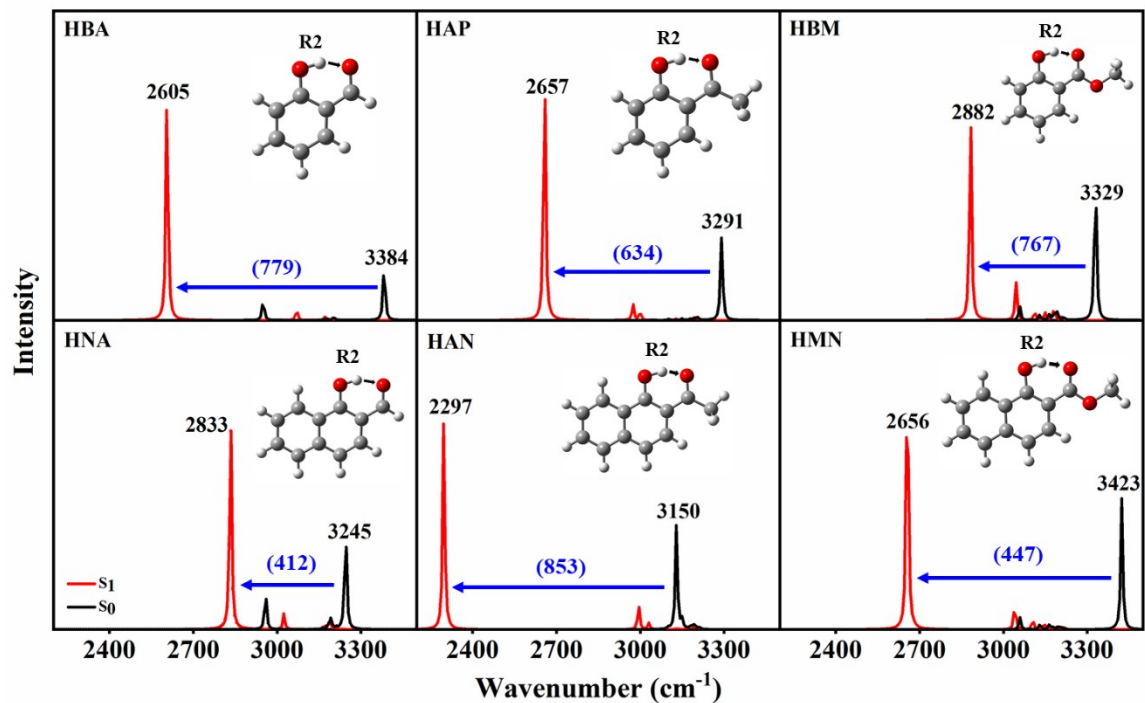
State	Bond	Wavenumber (cm <sup>-1</sup> )					
		HBA	HAP	HBM	HNA	HAN	HMN
S <sub>0</sub>	R2	3384	3291	3329	3245	3150	3423
S <sub>1</sub>		2605	2657	2882	2833	2297	2656
Δv		779	634	447	412	853	767

**Table S2** Vibrational frequencies of the R2 and R4 stretching vibrations involved in PT process of di-PT-type both in S<sub>0</sub> and S<sub>1</sub>.

Di-enol form								
State	Bond	Wavenumber (cm <sup>-1</sup> )			Bond	Wavenumber (cm <sup>-1</sup> )		
		DHNA	DHAN	DHNA		DHNA	DHAN	DHNA
S <sub>0</sub>	R2	3016	2849	3151	R4	3632	3611	3632
S <sub>1</sub>		2368	2624	2761		3315	3316	3364
Δv		648	225	390	Δv	317	295	268

Mono-ketoform								
State	Bond	Wavenumber (cm <sup>-1</sup> )						
		DHNA	DHAN	DHNA		DHNA	DHAN	DHNA
S <sub>0</sub>	R4	3733	3728	3727				
S <sub>1</sub>		2759	2785	2878				
Δv		974	943	849				



**Figure S2** Simulated IR spectra on O-H vibration mode of di-enol (EE) and mono-keto (EK) forms of di-PT-type in the spectral region of R2 and R4 stretching vibrational modes, respectively, both in the ground state (black line) and the excited state (red line).

**Table S3** Selected bond critical point parameters (in a.u.) related to IntraHBs (R1) involving the PT of enol form for mono-PT-type.

Compound	$\rho(r)$	$\nabla^2\rho(r)$	$V(r)$	$E_{HB}$	$G(r)$	$H(r)$	DI
HBA	0.077	0.146	-0.090	0.045	0.063	-0.027	0.172
HAP	0.082	0.152	-0.097	0.049	0.068	-0.030	0.179
HBM	0.074	0.148	-0.086	0.043	0.062	-0.025	0.162
HNA	0.064	0.136	-0.072	0.036	0.053	-0.019	0.151
HAN	0.072	0.141	-0.083	0.042	0.059	-0.024	0.165
HMN	0.062	0.134	-0.068	0.034	0.051	-0.017	0.141

**Table S4** Selected bond critical point parameters (in a.u.) related to IntraHBs (R1) involving the 1<sup>st</sup> PT of di-enol form for di-PT-type.

Compound	$\rho(r)$	$\nabla^2\rho(r)$	$V(r)$	$E_{HB}$	$G(r)$	$H(r)$	DI
DHNA	0.081	0.145	-0.094	0.047	0.062	-0.031	0.190
DHAN	0.081	0.147	-0.094	0.047	0.064	-0.030	0.184
DHMN	0.067	0.134	-0.075	0.038	0.054	-0.021	0.154

**Table S5** Selected bond critical point parameters (in a.u.) related to IntraHBs (R2) involving the 2<sup>nd</sup> PT of mono-keto form for di-PT-type.

Compound	$\rho(r)$	$\nabla^2\rho(r)$	$V(r)$	$E_{HB}$	$G(r)$	$H(r)$	DI
DHNA	0.051	0.144	-0.055	0.028	0.046	-0.010	0.168
DHAN	0.067	0.143	-0.077	0.038	0.057	-0.020	0.151
DHMN	0.062	0.145	-0.070	0.035	0.053	-0.017	0.140

**Table S6** The relationship between the PT barrier and the topological descriptor given in the BCP.

Topological descriptors	Difficult ESPT	Fast ESPT	Ultrafast ESPT
Energy barrier (kcal/mol)	> 6.92	0.0 – 6.92	Barrier less
$\rho(r)$ (a.u.)	< 0.051	0.051- 0.073	> 0.073
$\nabla^2\rho(r)$ (a.u.)	< 0.134	0.134 – 0.145	> 0.145
$V(r)$ (a.u.)	> 0.055	-0.086 to -0.055	< -0.086
$E_{HB}$ (a.u.)	< 0.028	0.028 – 0.043	> 0.043

G(r) (a.u.)	< 0.046	0.046 - 0.062	> 0.062
H(r) (a.u.)	> -0.010	-0.025 to -0.010	< -0.025
DI (a.u.)	< 0.140	0.140 – 0.162	> 0.162

**Table S7** Absorption band maxima of enol form ( $\lambda_{\text{abs}}$ ), emission band maxima of keto form ( $\lambda_{\text{emiss}}$ ), oscillator strength ( $f$ ) and major contribution (%) of all compounds calculated at TD-B3LYP/TZVP level.

Compound	Absorption (N)					Emission (T)		
	nm	eV	$f$	MOs (%contribution)	Exp.	nm	eV	$f$
HBA	315	3.941	0.067	HOMO→LUMO (95%)	328	504	3.029	0.041
HAP	314	3.956	0.084	HOMO→LUMO (95%)	-	458	2.704	0.084
HBM	293	4.236	0.094	HOMO→LUMO (94%)	-	429	2.892	0.096
HNA	358	3.462	0.084	HOMO→LUMO (94%)	368	402	3.081	0.076
HAN	350	3.539	0.108	HOMO→LUMO (94%)	365	396	3.127	0.106
HMN	332	3.738	0.102	HOMO→LUMO (92%)	342	371	3.340	0.105

**Table S8** Absorption band maxima of di-enol form ( $\lambda_{\text{EE}}$ ), emission band maxima of mono-keto form ( $\lambda_{\text{EK}}$ ), emission band maxima of di-keto form ( $\lambda_{\text{KK}}$ ), oscillator strength ( $f$ ) and major contribution (%) of all compounds calculated at TD-B3LYP/TZVP level.

Compound	Absorption (EE)				Emission (EK*)			Emission (KK*)			
	nm	eV	$f$	MOs (%contribution)	Exp.	nm	eV	$f$	nm	eV	$f$
DHNA	398	3.122	0.119	HOMO→LUMO (97%)	400	485	2.551	0.124	595	2.084	0.134
DHAN	387	3.213	0.152	HOMO→LUMO (97%)	-	473	2.617	0.171	594	2.084	0.171
DHMN	361	3.428	0.152	HOMO→LUMO (96%)	-	438	2.828	0.185	543	2.280	0.171

**Table S9** Maximum wavelength ( $\lambda_{\text{max}}$ ) of first excitation and deviation between the calculated and experimental wavelengths ( $\Delta\lambda$ ) for HBA and their derivatives calculated by various TD-DFT methods with TZVP basis set.

Compound	Method			Experiment (nm)	Reference
	B3LYP	LC-BLYP	CAM-B3LYP		
HBA	315	289	298	340	32
HAP	314	279	291	320	65
HBM	293	260	274	310	66
HNA	358	300	324	368	34
HAN	350	296	318	365	34
HMN	332	287	305	342	34

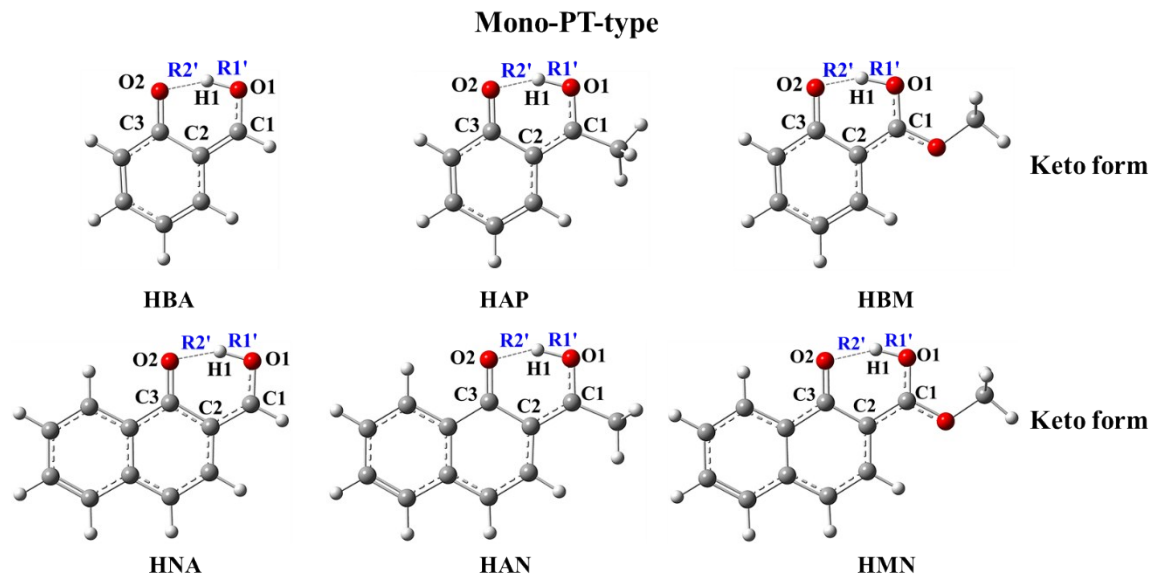


**Figure S3** Ground state optimized geometries of keto form of mono-PT-type in gas phase computed at B3LYP/TZVP level. Dashed lines represent intramolecular H-bonds and the important atoms involving PT process are labeled.

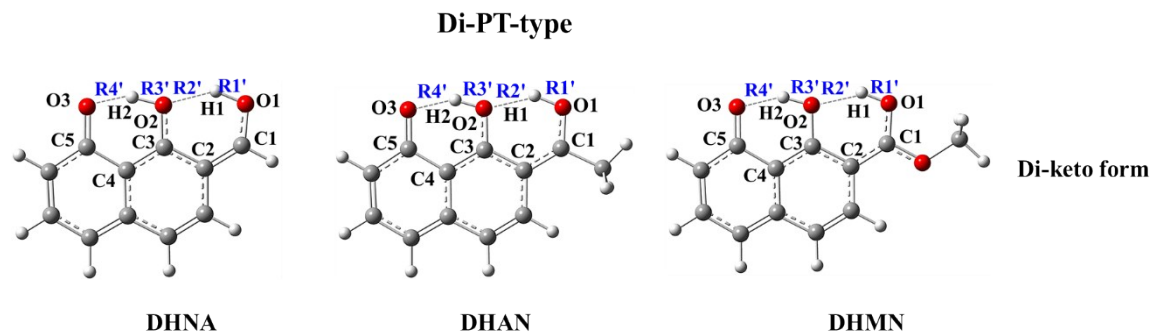


**Figure S4** Ground state optimized geometries of di-keto forms of DHAN and DHMN in gas phase computed at B3LYP/TZVP level. Dashed lines represent intramolecular H-bonds and the important atoms involving PT process are labeled.

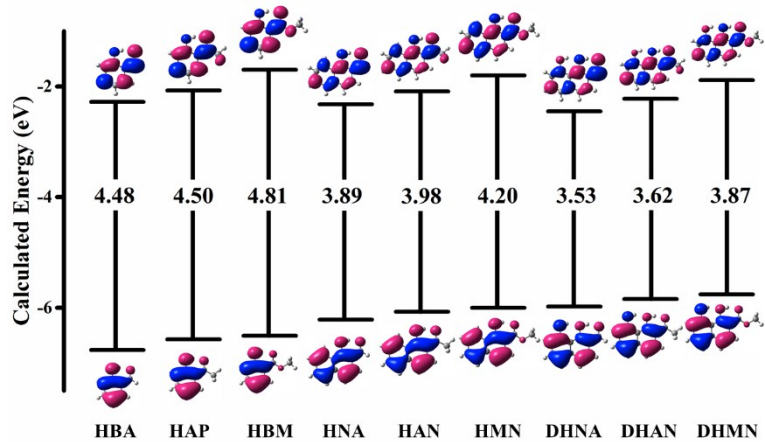


**Figure S5** Diagram of calculated HOMO and LUMO energy levels as well as HOMO-LUMO gaps (eV) and frontier molecular orbitals (MOs) of enol absorption of mono-PT-type and di-enol absorption of di-PT-type.

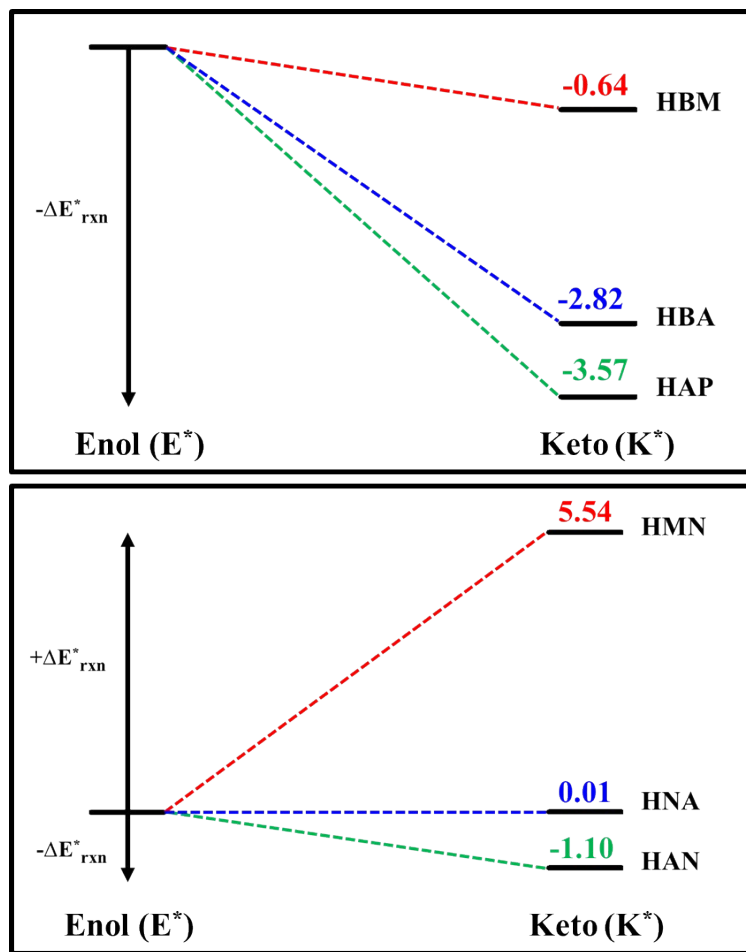


**Figure S6** The PT reaction energy in the  $S_1$  state ( $\Delta E^*_{rxn}$ ) of mono-PT-type computed from the energy differences between the optimized excited-keto and excited-enol forms ( $\Delta E^*_{rxn} = E^*_{keto} - E^*_{enol}$ ).

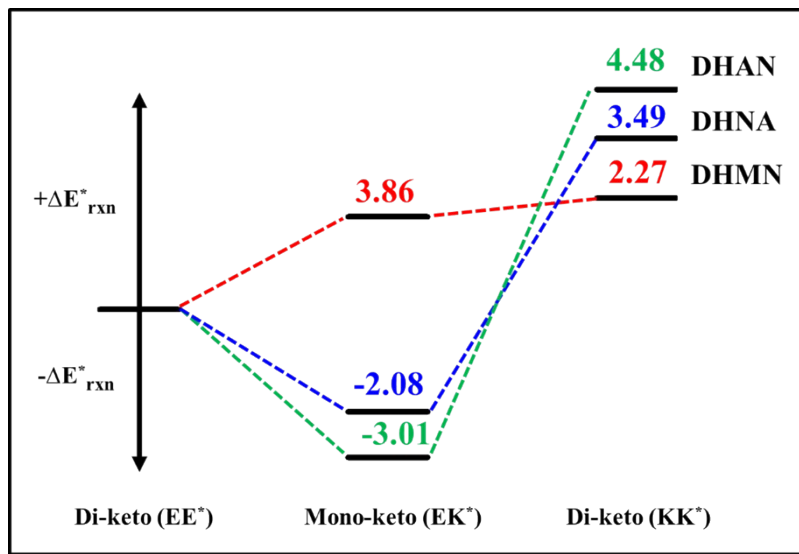


**Figure S7** The PT reaction energy in the  $S_1$  state ( $\Delta E^*_{rxn}$ ) of di-PT-type computed from the energy differences between the optimized excited-keto and excited-enol forms ( $\Delta E^*_{rxn_a} = E^*_{\text{mono-keto}} - E^*_{\text{di-enol}}$  and  $(\Delta E^*_{rxn_b} = E^*_{\text{di-keto}} - E^*_{\text{mono-keto}})$ .

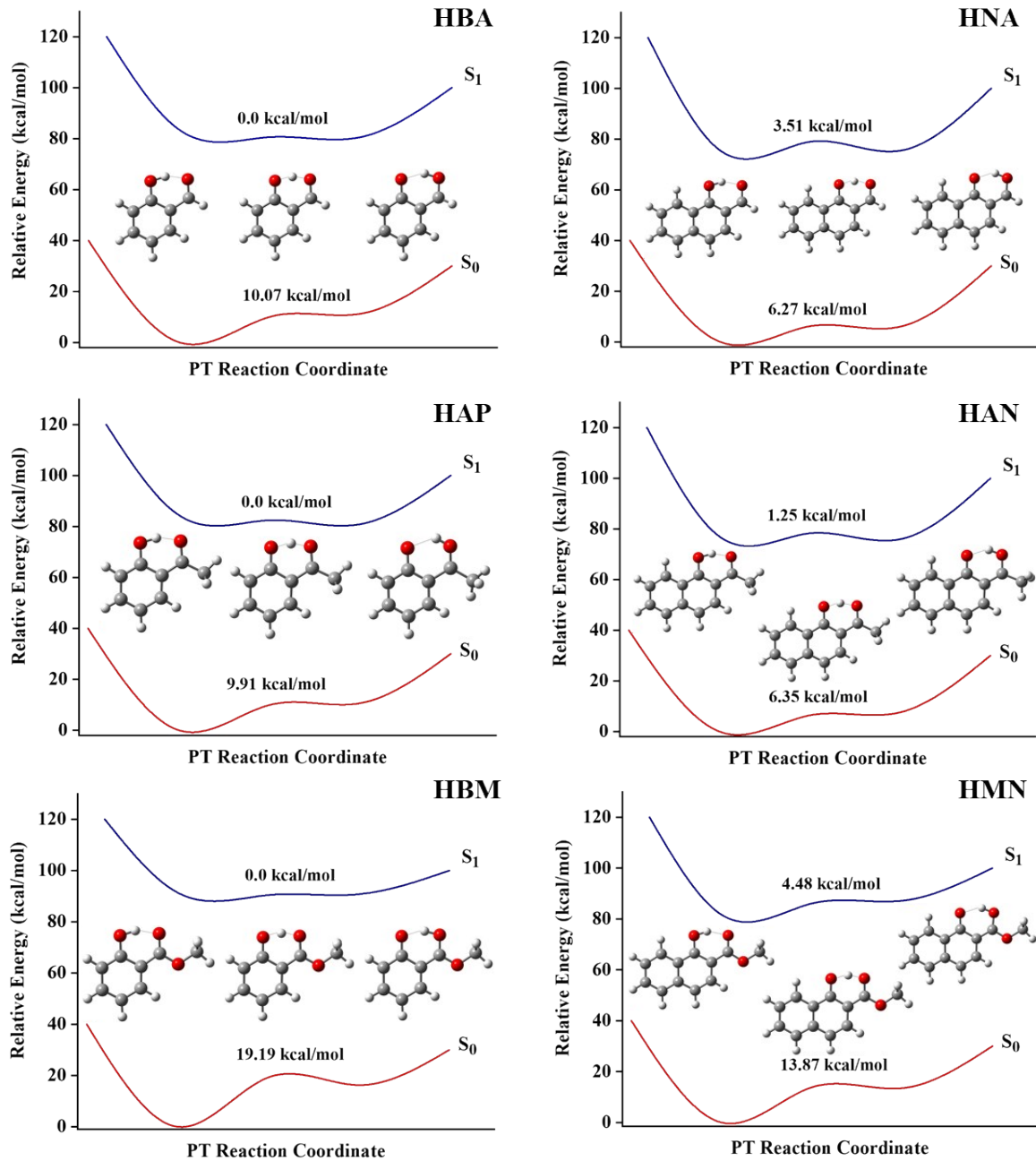


**Figure S8.** The potential energy curves (PECs) of PT reactions both in the S<sub>0</sub> and S<sub>1</sub> states of mono-PT-type computed at TD-B3LYP/TZVP level.

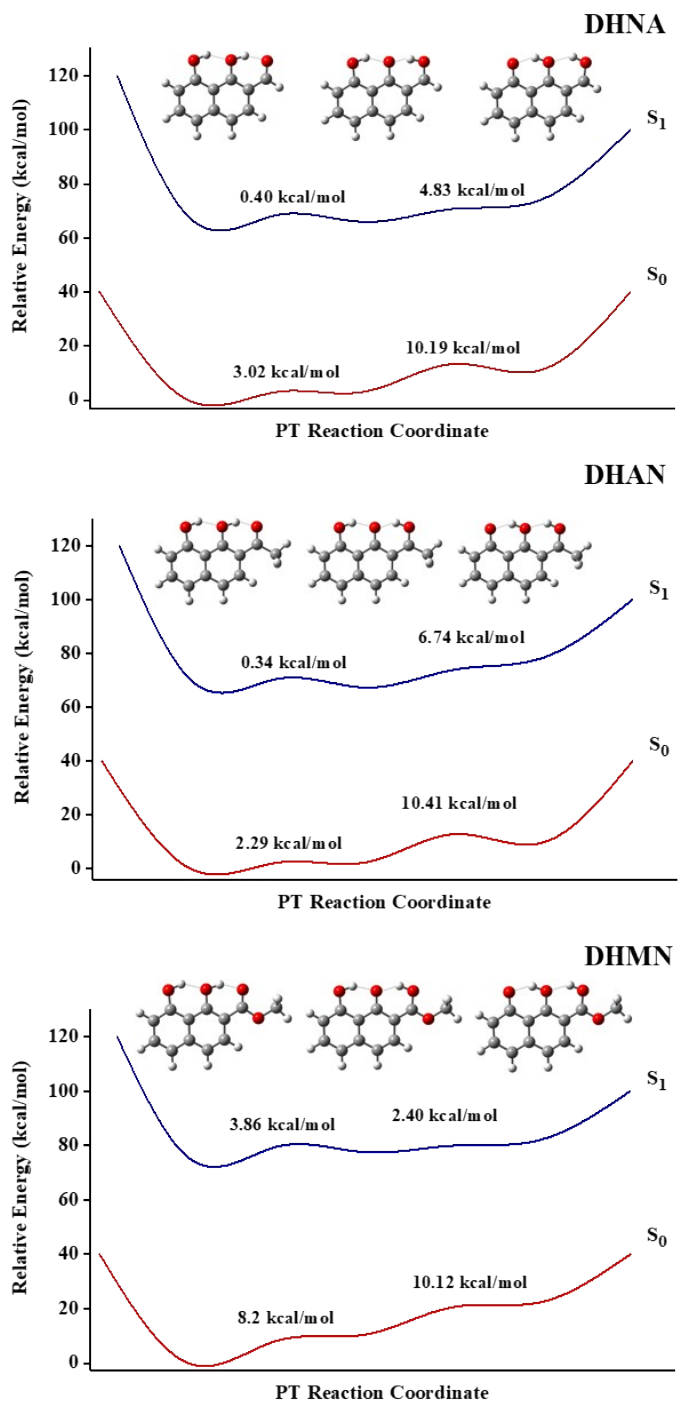


**Figure S9.** The potential energy curves (PECs) of PT reactions both in the  $S_0$  and  $S_1$  states of di-PT-type computed at TD-B3LYP/TZVP level.